Geomech. Geophys. Geo-energ. Geo-resour. (2020) 6:52
https://doi.org/10.1007/s40948-020-00175-9

ORIGINAL ARTICLE

Field evaluation of flexible support system with radial gap (FSRG) under a squeezing rock condition in a coal mine development

İbrahim Ferid Öge

Received: 22 February 2020 / Accepted: 31 July 2020 / Published online: 13 August 2020

Abstract A wide range of alternatives is available to design a support system to stabilize an underground opening under squeezing conditions. An underground mine development was selected for the research where the underground openings reach to a depth of 1000 m and weak geological formations are present. The operational concerns in the mine development led to a shaft support design having a thick reinforced concrete with very high early strength while the decline was supported by a traditional support system in the squeezing ground. The rigid support in the shaft was typically capable of sustaining high ground pressure and stabilized the opening within negligible radial displacements. It should be noted that the design of the rigid system was straightforward and high early strength concrete had key importance in this case, however, it could only be applied in the shaft. The traditional support system for the decline was a light and conventional system, consisting of thin shotcrete layer, cable bolts and steel arches suffered excessive deformation as high as 60 cm or more. A light-flexible support system with a radial gap was developed for the decline in the same geological unit, allowed substantial ground deformation to occur in a controlled manner, eventually, the opening was stabilized. The newly adopted radial gap allowed improved ground relaxation and reduction of the ground pressure acting on the secondary support layer. The design and application of the yielding support system with a radial deformation gap was effortful, hence the system can be used where available equipment and operational factors force practitioner to use a light and flexible system. The significance of the new system arises from keeping the ground support elements and the operation cycle the same while modifying the support design and installation procedure.

Keywords Squeezing ground · Rigid support · Yielding support · Rock deformation · Rock support

İ. F. Öge (✉)
Department of Mining Engineering, Muğla Sıtkı Koçman University, Muğla, Turkey
e-mail: feridoge@mu.edu.tr

1 Introduction

The rock mass behaviour around an underground opening is governed by the mechanical properties of the intact rock, discontinuities and their pattern, orientations and, the stress state around the underground opening. In fact, the relationship between the stress state and mass strength of the rock is one of the biggest factor governing the stability and deformation. If there is an unfavourable relationship between stress and strength, it is commonly called as a stress-related problem. Stress-related problems cover different types of rock failure. The rock strength range varies from deformable weak rock to brittle strong rock with violent and instantaneous failure tendency; the latter one is commonly pronounced as rock burst behaviour (Zhang et al. 2018) while the former one may exhibit squeezing behaviour. The squeezing failure is sometimes mistakenly interrelated with swelling behaviour. Swelling is observed where the rock or soil mass contains a considerable amount of swelling clay minerals. Swelling occurs when its moisture content is increased by the introduction of water (Majumder et al. 2017; Jimenez and Racio 2011). Moisture in the atmosphere of the underground opening may also have an influence on the swelling behaviour. The adverse influence of moisture on the strength of moist-sensitive rock should not be accounted for swelling behaviour. In such a case, considerable strength reduction can be observed and consequently, the rock mass may deform substantially. Although the presence of clay is a strong motive for squeezing ground, it may not always cause swelling failure. Another failure type in the underground openings is structurally controlled behaviour of the rock mass which is governed by the density and the orientation of the discontinuities as well as the strength-stiffness parameters of them. The opening shape, size, excavation method and support scheme can also be accounted for the deformation and stability of the underground opening. Groundwater inflow and pressure has also a great influence on the deformation and stability characteristics of an opening, so does the operational issues (Stille and Palmstrom 2008). Under a great water inflow and pressure, it may not always be possible to maintain face advance and the water inrush must generally be expelled by any means such as grouting or drainage measures. Apart from the deformation of underground openings, there may be negative effects of mining process to the environment (Vishwakarma et al. 2020).

Hoek (2001) takes the ratio of rock mass strength to in-situ stress into account in order to predict the deformation tendency associated with squeezing behaviour. In another approach, the parameter N, opening span, and depth parameters can be used for the prediction of the squeezing conditions. Here, N value is based on Q-System when the parameter SRF is equal to unity (Goel et al. 1995). Apart from the empirical studies, numerical modelling can also be employed for understanding the mechanism of the squeezing behaviour (Guan et al. 2018).

The support elements can be subjected to abnormal rock pressure in squeezing conditions. In such cases, resisting against deformation can be satisfied difficultly. The support design perspective for squeezing ground conditions can be basically divided into two concepts. The traditional one is a rigid support concept which can be regarded as a stiff and heavy support system which is expected to resist against high ground pressure (Barla 2001). Reinforced concrete, thick concrete or segmental linings can be accounted for rigid supports (Mezger et al. 2017). Another option is to construct a load-bearing stiff arch by using shotcrete. A thick layer of shotcrete can be combined with rebars to execute rigid support (Høien et al. 2019). Although persistent ground deformations are observed in a tunnel excavation case, using a heavier support system and increased construction quality can lead to a positive solution to the squeezing ground (Cao et al. 2018. It must be noted that the support failure is not the only negative consequence of squeezing. Jamming of TBMs poses a challenge against rapid tunnelling process (Zhang and Zhou 2017).

Another support concept is called as yielding or flexible support which allows some deformation to occur in a controlled manner by the dissipation of deformation energy in order to reduce the ground pressure and cause the relaxation of ground stress. Generally, the allowed deformation should be limited to a predetermined extent. The flexible support systems can be formed by several elements. The conventional one is yielding steel arches which are called as TH type steel supports. They allow the axial load on the support to be dissipated by a sliding action along with the clamped connections (Barla 2001). Compressible stress controllers are made of different materials which are used together with conventional support elements such as shotcrete and steel supports (Tian et al. 2016; Mezger et al. 2018). Even lattice girders and shotcrete can be designed in a form that they can be regarded as yielding and flexible support. Adoption of recently developed yielding support elements to tunnelling together with the behavioural analyses are presented in Barla et al. (2011). Cable bolt is another strong tool to deal with severely deforming ground (Shen 2014). According to Cantieni and Anagnostou (2009), the yielding pressure of a flexible support system is critical for appropriate ground relaxation and accommodation of support to the deformation. Low yielding support pressure may deteriorate the rock mass and it promotes loosening.

A high yield pressure is desired for increased performance of the system.

In this research, a shaft and a decline (inclined mine roadway) cases were taken into consideration. Both openings were driven through the same geological formations. At around the depth of 700 m, both excavations passed through a geological unit having a tendency to exhibit squeezing behaviour. Simply, high stress to rock strength ratio caused the deformation of underground opening in squeezing manner. The shaft was sunk and supported by a heavily rigid system while the decline was supported by a combination of shotcrete, cable bolts and steel arches. After encountering excessive deformation of traditional roadway support, a new flexible and yielding support was proposed. Although the same support elements were used in the new system, the introduction of radial gap to the system is the major contribution to the system. The new system has initial, intermediate and final layers. The initial layer was o combination of cable bolts, wire mesh and shotcrete. The final layer was constructed by using TH type steel arches and an additional layer of shotcrete. There was an intermediate layer between initial and final layers as a deformation gap which turns the system into highly flexible support. The proposed flexible support system with a radial gap was employed in the problematic chainages in the decline. The performance of the system was evaluated and presented in this research.

2 Study area and geological information

The research area is located at Soma Coal Basin in Manisa and İzmir, Turkey. A state-owned open cast mine is present in the northern region of the Soma Coal Basin where the coal seam lies at a shallow depth. Underground coal mines are under operation at a depth between 150 and 400 m and they are located at the south of the open cast mines (Öge et al. 2019). The mines in the basin are major coal producers of Turkey with relatively high calorific value. New underground coal mines to be operated by private companies with greater mining depth from 700 to 1200 m are in planning or development stages and at an approximate distance of 5 km from the currently operating mines (Öge 2018). The research was carried out in the deepest mine of Turkey. The lithology, location, and general view of the mine is presented in Fig. 1.

The coal-bearing stratum is called as Soma Formation and it starts with a basement conglomerate unit, overlying discordantly the metamorphic rocks. The conglomerate contains grey coloured, fine-medium sized grains cemented with sand and silt. A lignite zone with a thickness changing between 3.5 m and 30 m overlays this basement detritus, symbolized with M1. Known as KM2 in the regional Neogene nomenclature, this lignite is generally hard, massive, black, and bright appearance. The lignite quality decreases at the lower sections of KM2 whereas its clay ratios increase. A bluish/creamish-grey marl level (M2) overlays KM2 zone. Brinkmann and Feist (1970) combined this lithology, defined as M2 with upper limestone level (M3) and determined that both marl and limestone together could be called "marl-calcareous series". The marls are grey, greyish-green coloured, hard, and massive. The marl series (M2) were almost present at all of the boreholes drilled in the licensed area, thus it can be stated that it is widespread and homogenous. A Pliocene-aged formation named as Deniş is underlain by the coal-bearing Miocene-aged Soma formation. The Deniş Formation contains clastic limnic deposit succession with coal intercalations. The unit was sub-classified in six series by Nebert (1978). They are sandstone, siltstone and green–red clay level (P1), upper lignite level (KP1), clay-tuff-marl series (P2ab), clay-sandstone-conglomerate level (P2c), finely gravelled (siliceous) calcareous level (P3) and tuff-agglomerate (P4 or Plvt) levels. Here KP1 coal has no economic value. Here the coal seam lies at a 1000 m depth which may alter gas sequestration and permeability (Perera et al. 2011).

3 Underground openings and rock mass

Two shafts each having single inset at an elevation of - 570 m were completed. The ultimate depth of the shafts from the surface is more than 800 m. A decline roadway having a total length of $\sim$ 3500 m was driven and the depth of cover varied with respect to topography and inclination of the roadway. Both openings passed through P1 geological unit at an approximate depth of 700 m. The geological cross-section around the P1 geological unit for decline opening is given in Fig. 1. Numerous discontinuities and a few strike-slip faults with vertical throw were

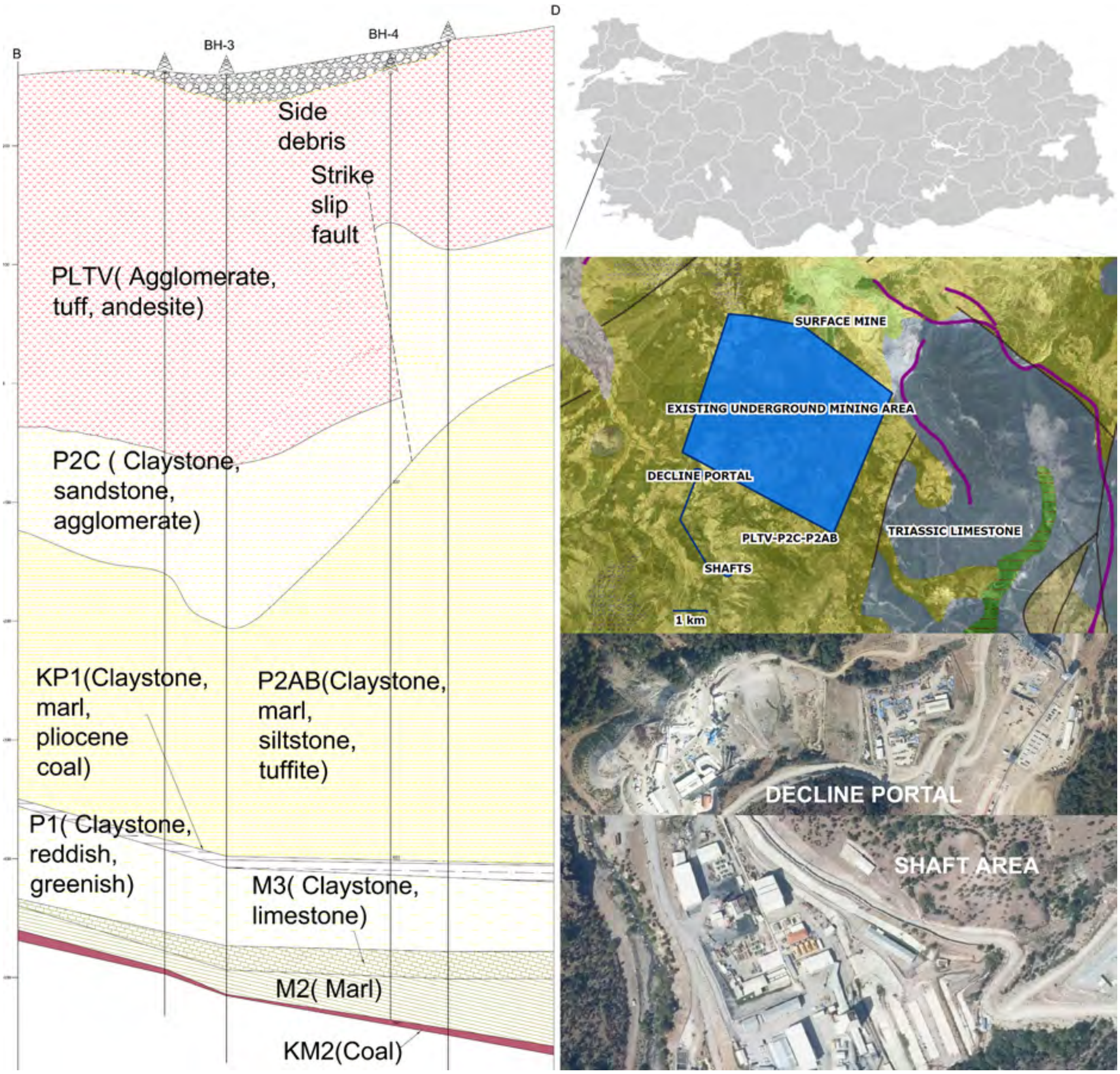

Fig. 1 Lithology, location, and general view of the study area (modified from Öge (2017) and MTA

encountered. In Fig. 1, the visual appearance of the P1 geological unit at the face and core boxes are provided. P1 siltstone with claystone unit is in the form of rock when it is carbonated while some sections are formed in soil-like form. Briefly, P1 unit can be described as a rock mass having very weak to moderate strong intact strength (According to the Ulusay and Hudson (2006), strength classes from R0 to R2) and this variation is clearly presented in the core boxes given in Fig. 2. The thickness of high and low strength zones is variable from tens of centimetres to meters. Bedding planes exist in the form of gradual transition. The fissured structure with slickensided discontinuity surfaces and dominantly weak intact rock strength can be observed frequently. The fissures suggest that the rock unit was subjected to tectonic influence. Discontinuity orientations are shown in a stereo plot for P1 section, however, the abovementioned internal fissures are disregarded since they are densely populated and irregularly oriented. The faults have an almost vertical dip and they are striking NW, hence, there is an acute angle between fault planes and decline face. Some of

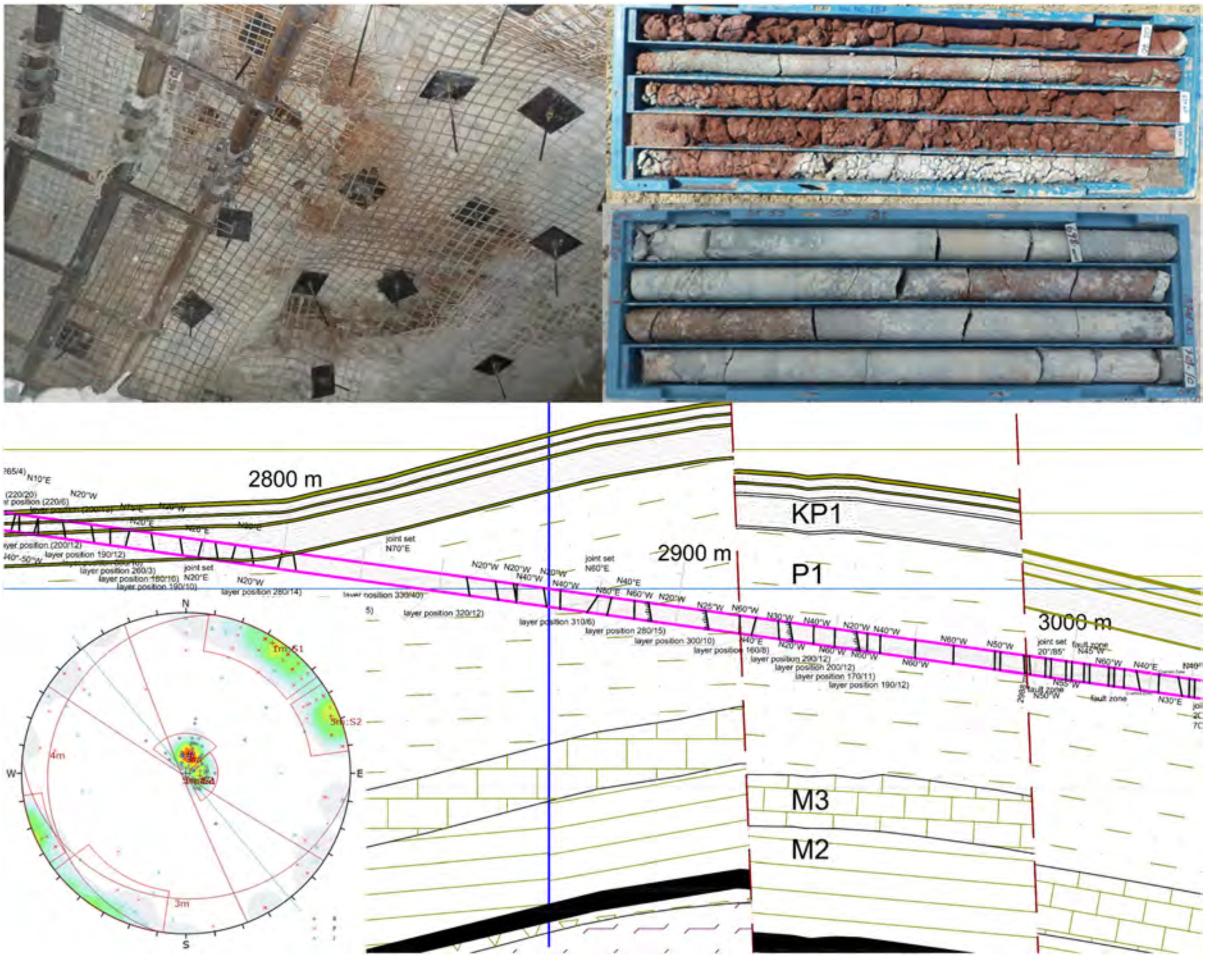

Fig. 2 Visual appearance of the rock mass in the decline and in the core boxes (top), geological cross-section, geological units around the decline and stereo plot of the discontinuities

the joints have a similar orientation with the faults while some of them are oriented randomly. Bedding planes dip amount vary between 6° and 25° under the influence of tectonic disturbance and dipping towards South, South-West and West. The geological conditions encountered along the decline is almost the same as the shaft area. The distance of P1 chainages between the shafts and the decline is approximately 250 m.

Although the borehole data was available, the rock mass classification data directly obtained from the decline was processed in order to acquire RMR (Bieniawski, 1989), Q-System (Barton et al., 1974) and GSI (Geological Strength Index) (Hoek 2002) values. The decline chainages located in P1 and KP1 are considered in rock mass data and presented in Fig. 2. It should be noted that the uniaxial compressive strength tests were carried out on regular samples while the ones in disturbed form could not be tested. Such soil-like P1 sections are clearly presented in Fig. 2 and the strength of these sections lie around 1 MPa. In Fig. 3, the dominant rating is illustrated by the solid line while the dashed line represents minor zones at a particular chainage. The rock mass classification ratings exhibit a variation at a certain chainage. It must be reminded that the rock mass is impervious along this section and resulted in positively high groundwater ratings for RMR and Q. Considering the RMR rating, dry rock condition contributes to the rating as high as 15. The rest of the RMR rating represents the structural quality and the intact strength of the rock. Considering Q-System,

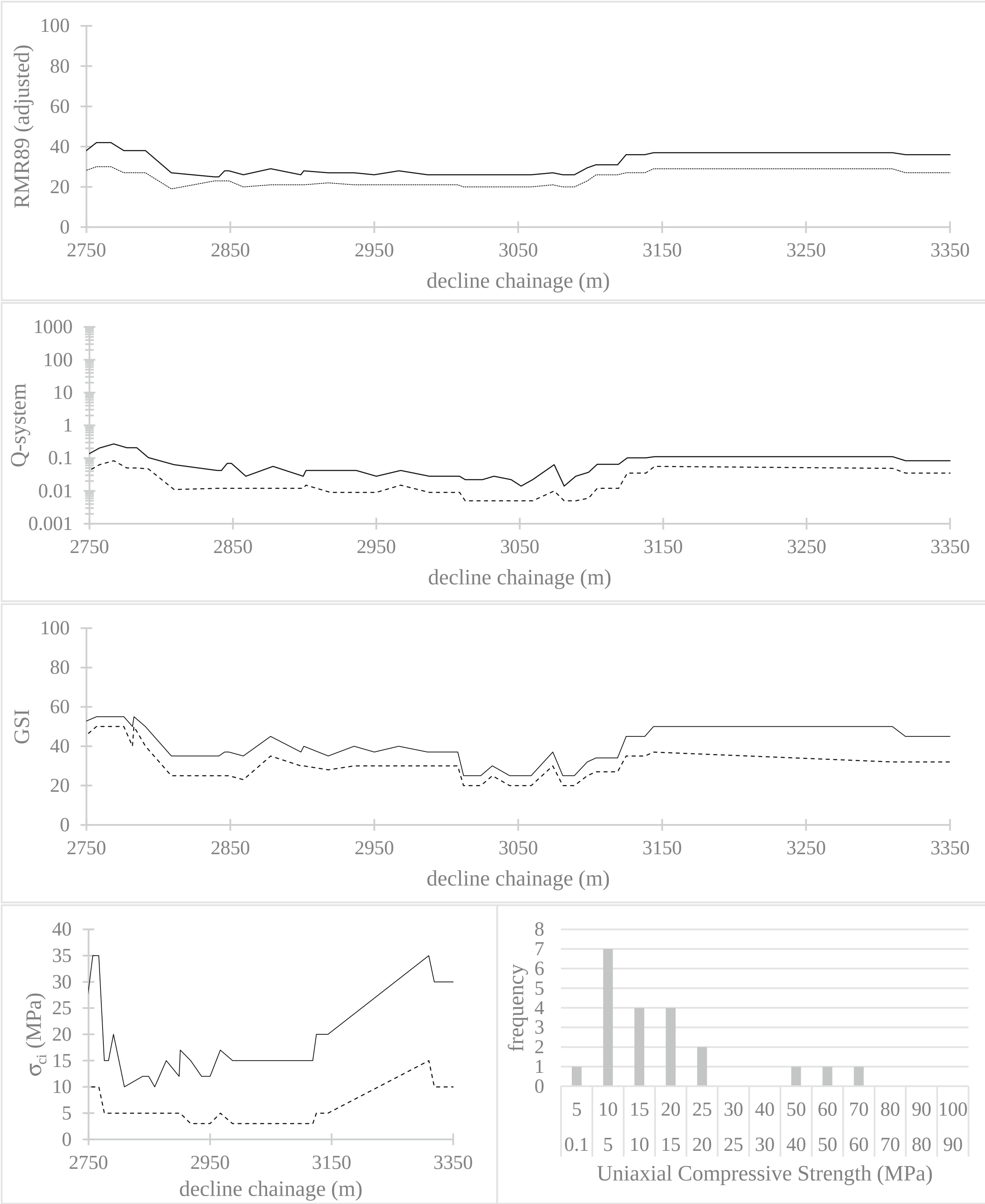

Fig. 3 Rock mass classification ratings, uniaxial compressive strength estimates collected at decline face and frequency histogram of the uniaxial compressive strength test results

tunnelling quality is found to be extremely poor and GSI ratings urge about the variation of the structural quality of the rock mass. Around 2750 m chainage there is a contrast in the intact rock strength arising from the relatively hard marl bands and weak coal seams existing in KP1 horizon. Along the P1 section, the strength data becomes more consistent.

The mechanical properties were selected based on the available laboratory test results of the P1 unit and on-site behaviour of the underground openings. Triaxial compressive strength tests were carried out on relatively stronger sections as expected. Unfortunately, soil-like and disturbed parts occupied a considerable percentage in the drill cores. Recovery of regular core samples was difficult due to the weak nature of soil-like sections. In fact, the weak nature of the soil-like sections could be deeply examined by taking grain sizes into account (Wasantha et al. 2015), however, it was not possible at that time. Gen.Hoek–Brown parameter m_i varies between 7 and 43 among 4 sets of triaxial compressive tests with a majority between 7 and 14. The borehole drillings were carried out along the shaft axes and 21 uniaxial compressive strength tests were carried out. Gen. Hoek–Brown parameters for P1 geological unit, in general, were estimated by assigning a GSI rating to 50 for peak and 25 for residual strength. Peak and residual parameters were given in Table 1 together with rock mass elastic modulus (E_{rm}) which was calculated by the method proposed by Hoek and Diederichs (2006). The equivalent cohesion (c') and internal friction angle (ϕ') of the materials were also given just to inform the reader but not used directly in any analysis. As a common simplification, relatively strong and weak rock sections were treated as a homogenous, isotropic material and represented by “P1 or KP1” material. Strong (P1 strong) and weak (P1 weak) sections were also treated separately and corresponding parameters were shown in Table 1.

In order to assess the squeezing condition, several approaches can be used. Approximated depth, in this case, was 700 m and rock mass strength, σ_{cm} was around 2.33 MPa, or sometimes even smaller (Hoek et. al 2002). The ratio of rock mass strength to in-situ stress was considered in Hoek’s (2001) approach. The ratio was around 0.14 and according to the approach, extreme to very severe squeezing conditions would be encountered. Goel et al.’s (1995) approach was based on Q-System parameters. The parameter N was used for the stability evaluation and SRF parameter was taken as 1 for the calculation of the parameter N. Even for a Q rating equal to 0.04 and SRF = 10, the approach foresees high squeezing at a depth greater than 374 m. Taking both approaches into account, it was concluded that the ground behaviour was squeezing with a significant margin.

Another point was the in-situ stress state in the study area. Due to the weak nature of the intact rock and densely spaced discontinuities in the mass, any in-situ stress measurement technique could not be employed. In such rock masses, a direct measurement was somehow difficult due to the core loss in overcoring. Establishment of smooth borehole surfaces was another concern, which was not possible in weak and fractured rock. Hydraulic fracturing might seem misleading due to the existence of natural fracture expansion during pressurisation. Relying on a single in-situ stress technique was also considered to be misleading. It is a well-known fact that the different techniques should be employed, and a cross-check among them is necessary in order to acquire reliable data. In the study area both the intact and mass strength values were found to be very low (1 to 15 MPa). In addition to the low intact material strength, the rock mass classification parameters, such as RMR89,

Table 1 Mechanical properties of the geo-material

Material	E_{rm} (MPa)	Gen. Hoek Brown (peak/residual values)				Equivalent Mohr–Coulomb	
		σ_{ci} (MPa)	m_b	s	a	c' (MPa)	ϕ' (°)
P1 or KP1	676	11	2.515/1.03	0.0039/0.00024	0.506/0.531	1.163/0.743	26.19/19.96
P1 strong	2198	15	4.110/0.824	0.0357/0.00024	0.501/0.531	1.671/0.764	32.20/20.25
P1 weak	139	1	4.682/2.74	0.1889/0.0357	0.500/0.501	0.581/0.451	14.66/12.09

Q-System and GSI ratings point out very weak classes. Considering the weak nature of the rock mass, it can be concluded that sustaining a high stress differential might not be possible for the weak rock. Assuming a vertical to horizontal stress ratio was very close to the unity could be reasonable and it was applied in the analyses (Hoek 2007). The vertical stress was taken as a function of the depth and unit weight of the rock, traditionally.

4 Support applications in squeezing ground

In the mine shaft with an inner diameter of 8 m, the reinforced concrete support system was executed at a close distance to the shaft bottom. The support in the form of a complete circle exhibit heavy and rigid support characteristics. Contradicting to the shaft support, in the decline heading, cable bolts, shotcrete layer and yielding steel arches constituted far more yielding and flexible system. The dominant rock mass behaviour was squeezing, comparison of the shaft and decline was valid since the dead weight of loosened rock or structurally controlled failure played an insignificant and negligible role. This fact was verified during the excavation works that structurally controlled failure was not a case. The decline heading and shaft sinking were carried out without problems at the face, however, squeezing had a considerable impact on the stability of the openings. Initially, the applications were explained separately, later on, the rigid shaft liner as compared to flexible support with deformation gap. Another important comparison was made between the traditional yielding support system of the decline and the new Flexible Support System with Radial Gap (FSRG). It should be noted that the numerical modelling presented here was not carried rigorously, instead, the main focus was on the field behaviour. Some operational issues were also explained in detail to emphasize the influence of operational restrictions on the support design.

4.1 Application of traditional rigid shaft support

In general, being practical and ensuring operational simplicity is essential in mining operations. The reinforced concrete lining was preferred during shaft sinking in the study area considering operational concerns. Approximately after 5 m long drilling and blasting round in the shaft sinking cycle, the muck removal operation took place. After trimming the periphery, the operations went on with the installation of reinforcement bars. Later on, the concrete placement was carried out by using a retractable mould. Local rock bolting with wire mesh was applied where necessary to maintain desired opening size. Two reinforced concrete linings were planned in the section located in the P1 geological unit. The outer reinforced concrete liner had a 40 cm thickness with double reinforcement layers. The reinforcement bar spacing was 25 cm and the bar diameter was 25 mm. The outer support layer was considered as an initial support element and it would be overstressed during the hardening of the concrete. In order to satisfy long term durability, a second reinforced concrete layer was planned to have a thickness of 60 cm. The second layer would not be stressed initially, however, it could carry the load in case of the failure or deformation of the first layer by the time or when an additional deformation occurs. The inner concrete liner could be considered as a final lining and would be installed after the completion of the outer liner. The concrete standard was kept as high as possible since the liner was expected to be subjected to high stress due to weak ground conditions and early support installation. The strength variation with respect to the time is expressed by a logarithmic function as illustrated in Fig. 4. The average strength of the concrete is 32 MPa in 24 h while it is 45 MPa in 3 days. The concrete class can be indicated as C50/60 for the shaft lining. It must be kept in mind that this rheology is important for support design.

In order to analyse the support system, plane-strain and axisymmetric modelling techniques were used together. Although, the logic of the analysis was similar to the research presented by Vlachopoulos and Diederichs (2009), the pre-existing longitudinal displacement profiles (LDP) proposed by the researchers were not used. Instead, a basic axisymmetric numerical modelling was used for the construction of longitudinal displacement profile (LDP). The displacement profile with respect to the distance to the face was acquired by taking the LDP into account in unsupported case. This aspect is similar to the research presented by Vlachopoulos and Diederichs (2009). Later on, the analyses were pursued with plane strain analyses at concrete strength levels of 35 MPa and 50 MPa. The findings are presented by using LDP and

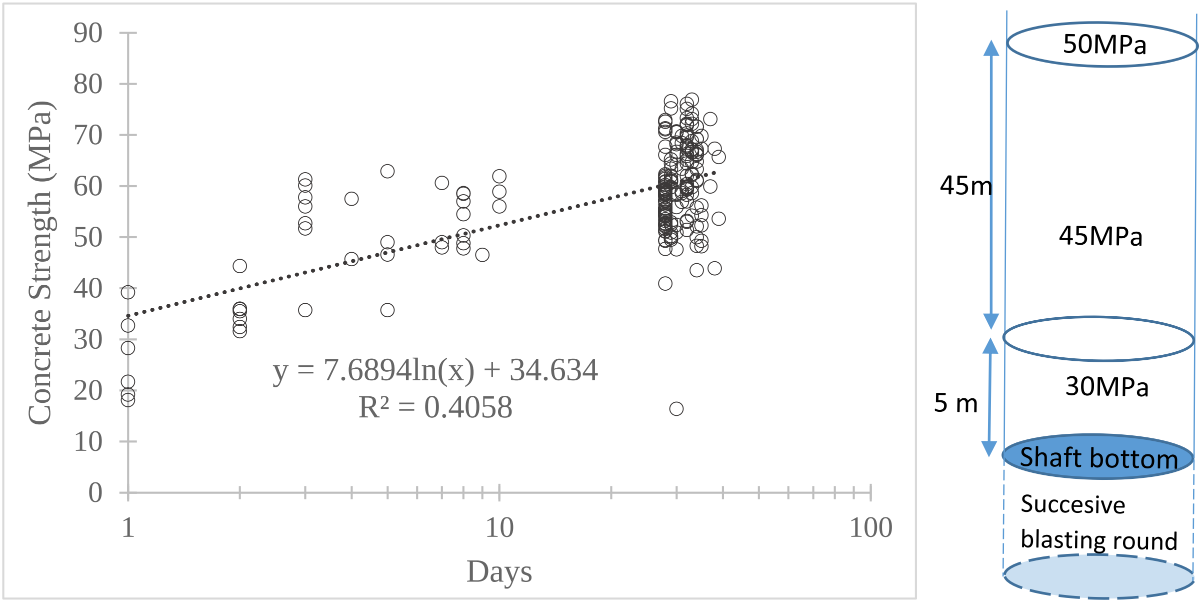

Fig. 4 Concrete strength evolution vs. time

Ground Reaction Curves (GRC) in Sect. 5 together with the comparison to the decline case. The parameters used in the analyses are given in Table 1.

The excavation diameter was 10 m for the shaft having an inner diameter of 8 m. The preliminary numerical modelling work was carried out by a Finite Element Analysis program (Phase^2 v.8 (Rocscience Inc. 2011)). The unsupported analyses resulted in the radial displacement of 1.9 m. Such modelling result was an indicator of squeezing ground conditions and the degradation of the rock mass around the shaft eventually leading to a total closure of the opening (Fig. 5). In case of the application of 40 cm thick reinforced concrete liner, the stress state of the liner was found to be stable during the early strength stage of the concrete. It must be noticed that the outer reinforced concrete layer had been subjected to high stress during early strength. In further hardening, the envelope in axial thrust-bending moment interaction diagram of the reinforced concrete expanded in the favour of strength-stress balance with a radial displacement around 3 to 5 mm.

The findings were compatible with field observations. No cracks or even hair cracks were observed on the shaft liner, however, the initial 40 cm thick reinforced concrete lining was calculated to be stressed close to its limits. Although the liner was substantially stressed due to the early installation of the support close to the shaft bottom, the opening was completely stable. In order to ensure long term stability and durability, 60 cm thick reinforced

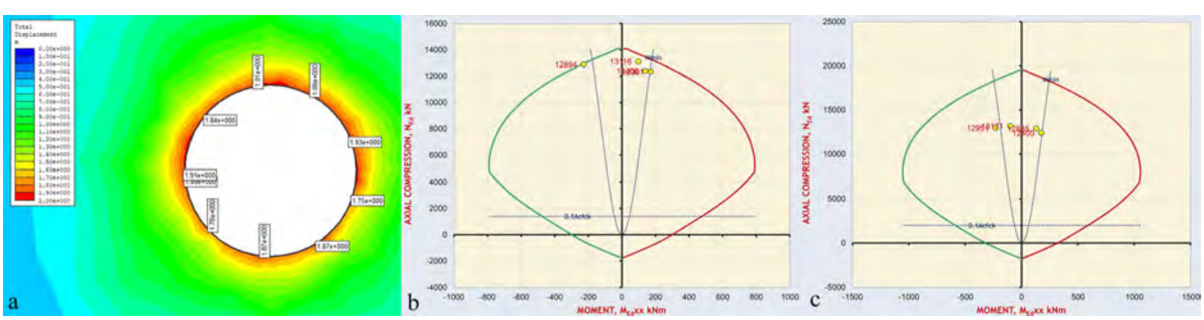

Fig. 5 Deformation potential of the unsupported shaft (**a**), interaction diagram of reinforced concrete in 24 h (**b**) and in 84 h (**c**)

concrete would be further placed, however, it was not considered in the analyses.

The 40 cm thick concrete has a support pressure of 2.72 MPa based on 24-h strength of concrete, and 4.25 MPa at 28 days hardening by using the method presented in Carranza-Torres (2004). The final lining has a support pressure of 6.22 MPa. Both the initial lining and final lining can be considered as a heavy and very stiff support system capable of resisting squeeze pressures, practically without deformation.

4.2 Application of traditional and new flexible support

Additional operational difficulties in underground mining excavations can be frequently encountered when it is compared to the civil tunnelling. Roadway heading at a high gradient can be accounted for the difficulties in mining operations. Sometimes, mining roadways are driven for a few thousands of meters at 1:4 gradient or even steeper. The waste removal and vehicle travel at down dip heading is a problem in cases where rubber-tired equipment was preferred. Rubber tired equipment use at a steep gradient can also be a problem from health and safety point of view. Typically in local coal mining operations, in order to ease waste removal operations, roadheader is integrated into a bridge and belt conveyor system (Kahraman et al. 2019). This integration limits the mobility of the roadheader by keeping it at a close distance to the face. Due to the presence of a roadheader having a width almost equal to the width of the roadway, mobile equipment used for shotcreting or bolting may not be located close to the face. In contrast to the roadway heading operations in the mining industry, in a large 3 lane highway tunnel heading, mechanisation can be highly flexible and a wide cross-section enable better mobility for the equipment.

Due to the abovementioned concerns, in this case, hand-operated drills were used for cable bolting and dry-mix shotcrete application was preferred at the face. All of which was accomplished after the roadheader advance. A mobile mould use was also considered for a final reinforced concrete final lining in the mine roadway in order to ensure long term stability of the opening, however, it was not preferred due to the operational concerns. These concerns involve the space occupied by the mould which obstructs monorail transportation, man and material passage as well as the pipes and belt conveyor, all of which should be actively running continuously. Instead, an increased thickness of shotcrete was considered as an alternative solution.

A traditional support system can be constructed by using several elements such as shotcrete with steel-fibres or wire mesh, cable bolts, steel arches. The typical support combination for fair to weak rock mass in the mine consists of 7 cm thick shotcrete with wire mesh, cable bolts (in a pattern from 0.75×0.75 m to 1.5×1.5 m) and steel arch spaced either 0.75 m or 1 m. Construction of the invert is generally neglected in order to keep advance at the desired rate. This system was not successful and easily deformed. A new system had to be developed in order to keep the roadway functional.

The proposed support system is given with respect to the installation sequence: #1: 15 cm thick shotcrete with steel fibres or mesh, #2: 6.3 m long resin grouted cable bolts in 0.75×0.75 m pattern with wire mesh #3: Installation of TH34 type yielding steel arches with a deformation gap. #4: A final 15 cm thick shotcrete layer. Invert construction can be accomplished behind the roadheader at a distance of 15–30 m to the face. A radial deformation gap is planned between shotcrete—cable bolted layer and steel arches (Fig. 6). The deformation gap allows full load mobilisation of the initial thin layer of shotcrete and cable bolt system during while the relaxation of the ground takes place partially. In fact, the gap size is determined by considering the support behaviour and ground deformability character by using several analysis methods. Those analyses will be presented further in this section. The deformation gap size is estimated to be around 30 cm. In practice, this value may vary due to the irregularities on the wall surface.

Initial layers provide a support pressure of 0.544 MPa while the final shotcrete layer and steel arches together satisfy a support pressure of 0.933 MPa. Further details are provided in Chapter 5 on the calculation of the support pressure values both for traditional support combination and proposed system.

According to the preliminary numerical analyses which were carried out in two different approaches, the required deformation gap size lies between 20 and 40 cm. Initially, the rock mass was simplified as an isotropic elastic-brittle-plastic material (Fig. 7, left).

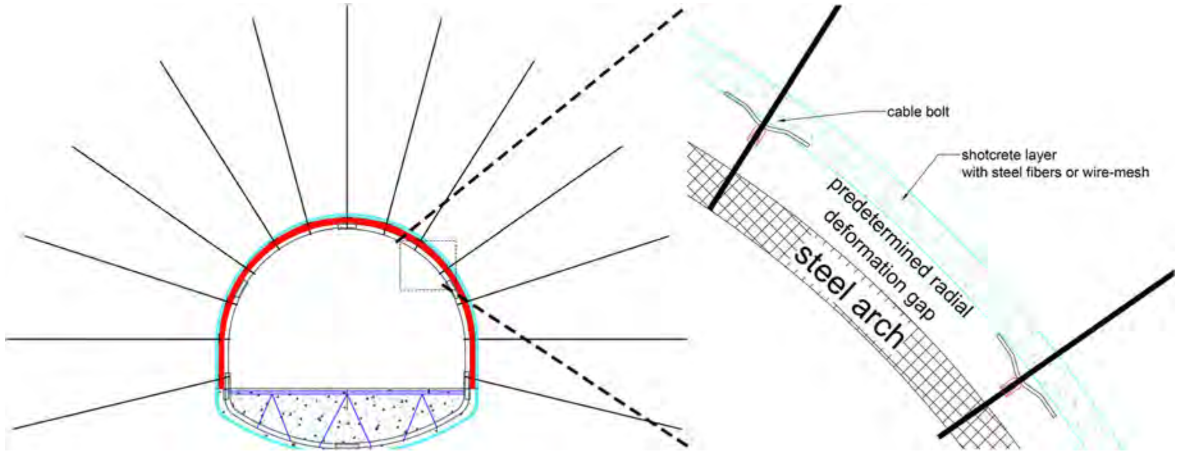

Fig. 6 Applied support system for decline with radial deformation gap (red coloured)

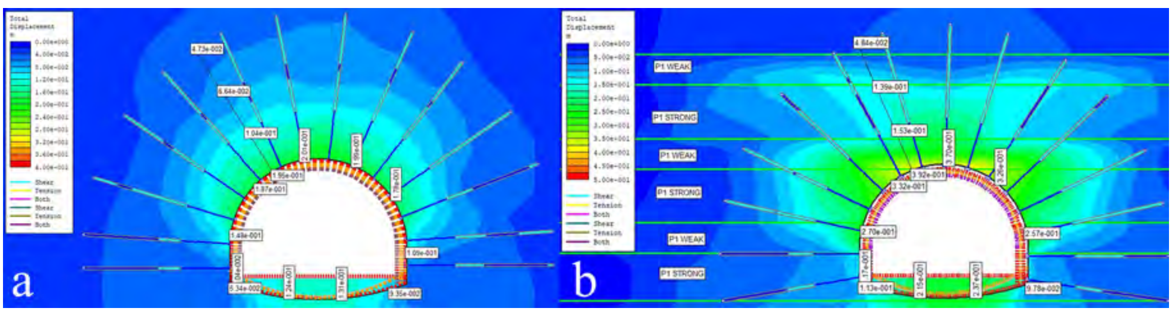

Fig.7 Deformation contours for isotropic elastic-brittle-plastic material (**a**) and strong and weak rock separate layers (**b**)

In the second approach, strong and weak rock layers were imposed on the model, separately (Fig. 7, right). The rock mass parameters are given in Table 1.

The simplified numerical analyses revealed that after the application of the final thick shotcrete layer, the support layers subject to a very small deformation, such as 1 cm. The field response of the proposed method was compatible with the findings acquired in numerical analyses, however, in particular sections, radial displacement amount reached up to 10 cm.

Along a considerably long section, previously mentioned support system was applied with several deficiencies, missing elements and delayed applications. The final and thick layer of shotcrete and invert construction was delayed for a long time and support circle was not closed for a long time. In fact, at a 150 m distance to the decline face, only initial 7 cm thick shotcrete, cable bolting and wire-mesh were applied immediately after the advance. Applied support pressure was less than 0.544 MPa and the missing support pressure was 0.933 MPa under these circumstances. It should be noted that the support pressure calculation is given in detail in Chapter 5. Consequently, the poorly supported decline section suffered considerable convergence up to a value of 20%. 64 stations were established along the problematic section of the decline and one of the convergence measurement is provided as a sample (Fig. 8). The measurements were taken for up to 7 times at the stations while some of the stations had only a few readings.

The initial deformation measurements (zero readings) were aimed to be taken almost at the face. This would allow capturing the cumulative deformation behind the face. However, some of the readings were calibrated due to having late zero readings (delayed initial readings). It must be noted that the pre-convergence occurring ahead of the face cannot be measured by total station measurements.

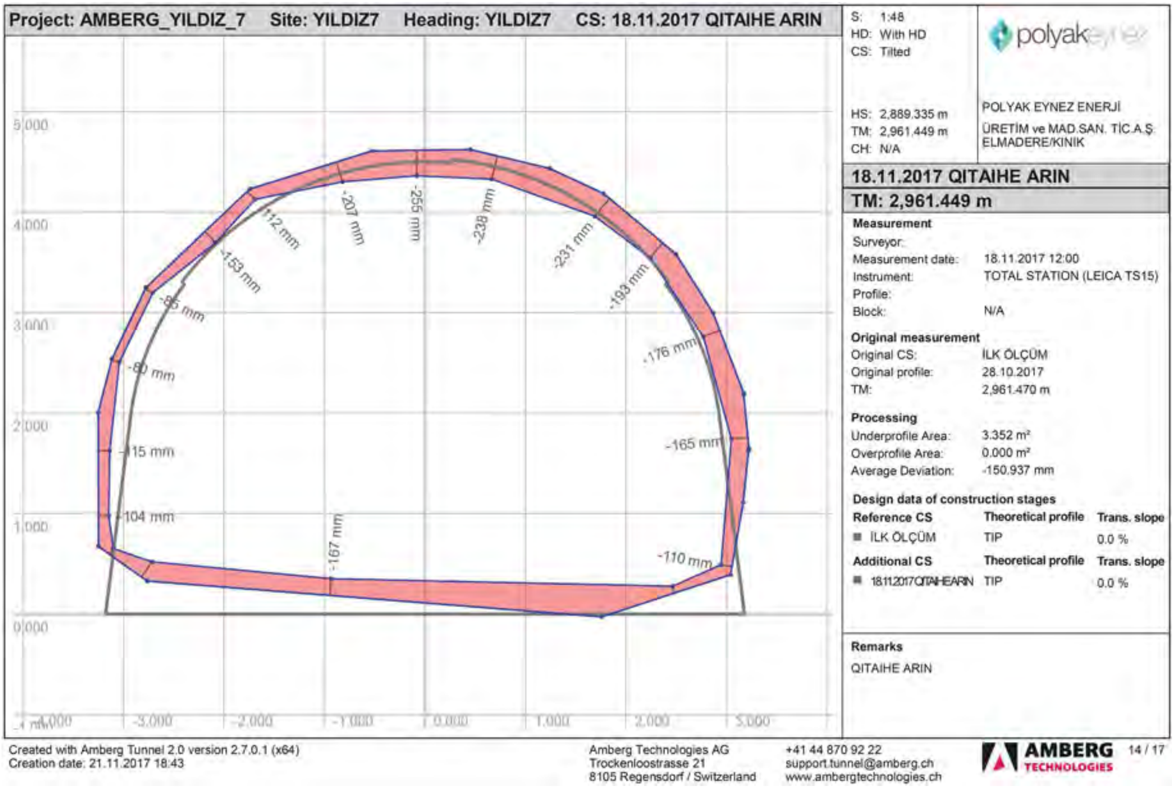

Fig. 8 Convergence measurement by using the total station at 2 + 961.5 m chainage

The deformation measurements along insufficiently supported decline segment are interpreted in Fig. 8. The details about the roof and side walls are shown in Fig. 9a–c. At the roof and the walls, the deformations could not be stabilised without the ring closure and final shotcrete lining. The deformation rate had an increasing trend at a close distance to the face (Fig. 8d). Eventually, it reached its maximum value at a distance between 75 and 120 m to the face. The whole deformation rate data was also presented with respect to the duration of each monitoring section. According to the Fig. 9e, after 40 days, the deformation rate started to decline down to 20 mm/day. This highly deformed segment was stabilised after the application of the final shotcrete layer and ring closure. Deficiency in support system without final shotcrete layer and invert was also obvious in cumulative roof and sidewall deformation readings.

5 Comparison among shaft liner, traditional and proposed roadway support system

The fact that it is essential to calculate maximum support pressure, elastic and post-failure stiffness of the support systems in order to determine the support reaction with respect to the radial deformation. For simple openings, such as, support elements in the form of closed circles, several analytical solutions exist but they are not repetitiously given here (Carranza-Torres 2004; Lowson and Bieniawski 2013). For a circular shaft opening, the solutions can be representative while it can be quite difficult to precisely achieve a result for horseshoe-shaped shotcrete and wire mesh support. Another concern is the mentioned analytical solutions cover a displacement range within the elastic limits while it is a must to construct a complete support pressure and displacement relationship. It is possible to install numerous load-cells or other load measuring devices to the support systems. In such a case, the number of radial load measurement devices will be limited. For each load or stress level, the

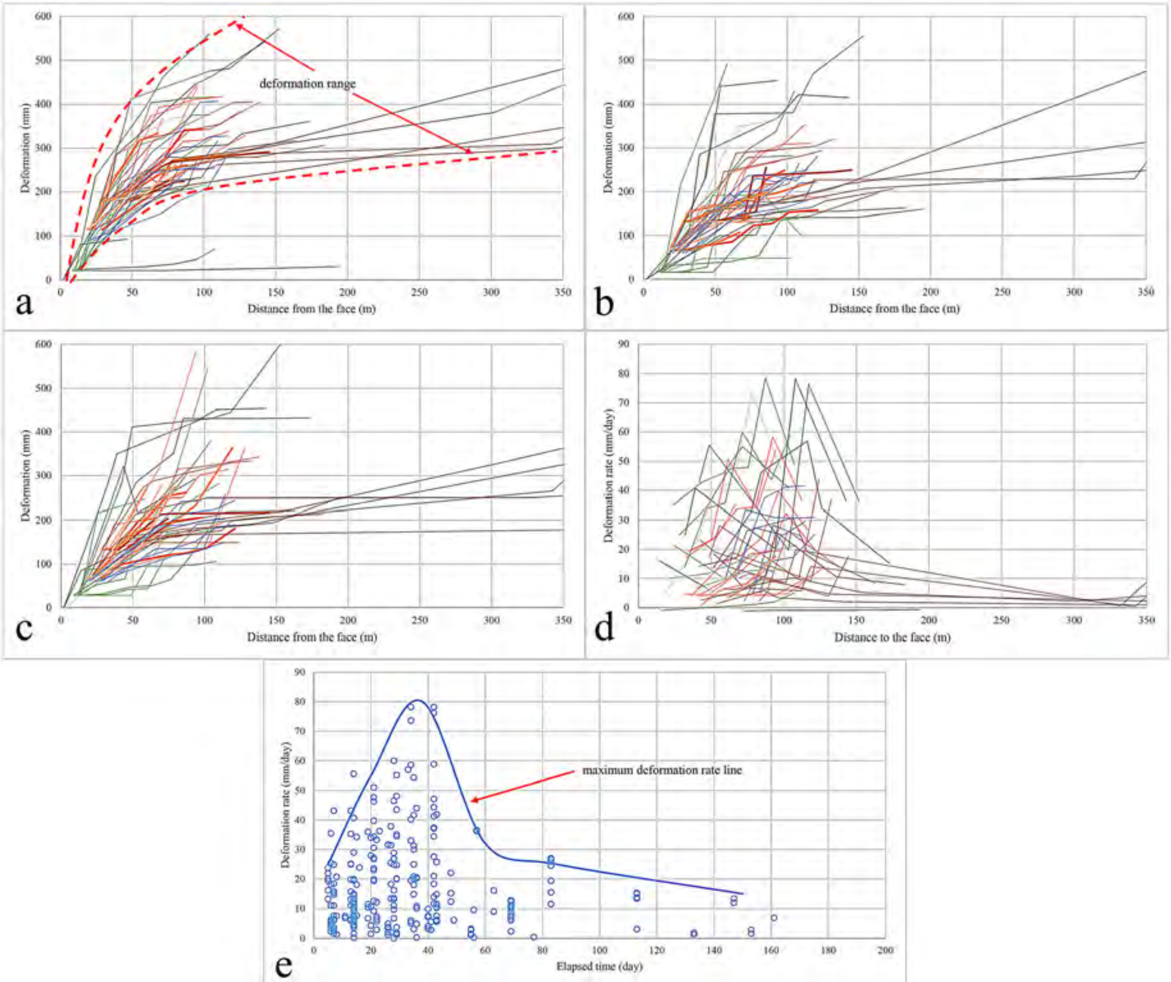

Fig. 9 **a** Deformation at the roof, **b** deformation at the left sidewall, **c** at the right sidewall, **d** deformation rate in mm/day with respect to distance to the face **e** deformation rate in mm/day with respect to the elapsed time after excavation

corresponding radial displacement must be measured. This fact makes such a measurement program almost impossible (at least for the time being) for tens of data sets as it is present in this research. An extensive effort and its results are given in research by Barla et al. (2011). In their research, a single special section was identified and detailed field behaviour of the rock mass around an opening was investigated. It can be seen that such detailed field instrumentation program may not be executed in numerous stations. Due to the reasons mentioned here, the support pressure – radial displacement relationship is constructed by making use of large scale support tests existing in the literature.

The maximum support pressure of shotcrete support relies on the concept of the supporting acting simply as an arch in compression. The basic formula for this type of support has been modified to reflect the realistic action of shotcrete and the construction process by Lowson and Bieniawski (2013). Their formulation is not only based on an arch in compression but also take bending resistance into account. Consequently, this approach results in a smaller support pressure than it is calculated by the analytical solution for circular concrete support under uniform loading (as it is presented in Carranza-Torres 2004). Support pressure ensured by 15 cm thick shotcrete with wire mesh is found to be 0.189 MPa by the modified approach. Another concern is again to derive support pressure as a function of radial displacement. When the energy absorption of shotcrete is of concern,

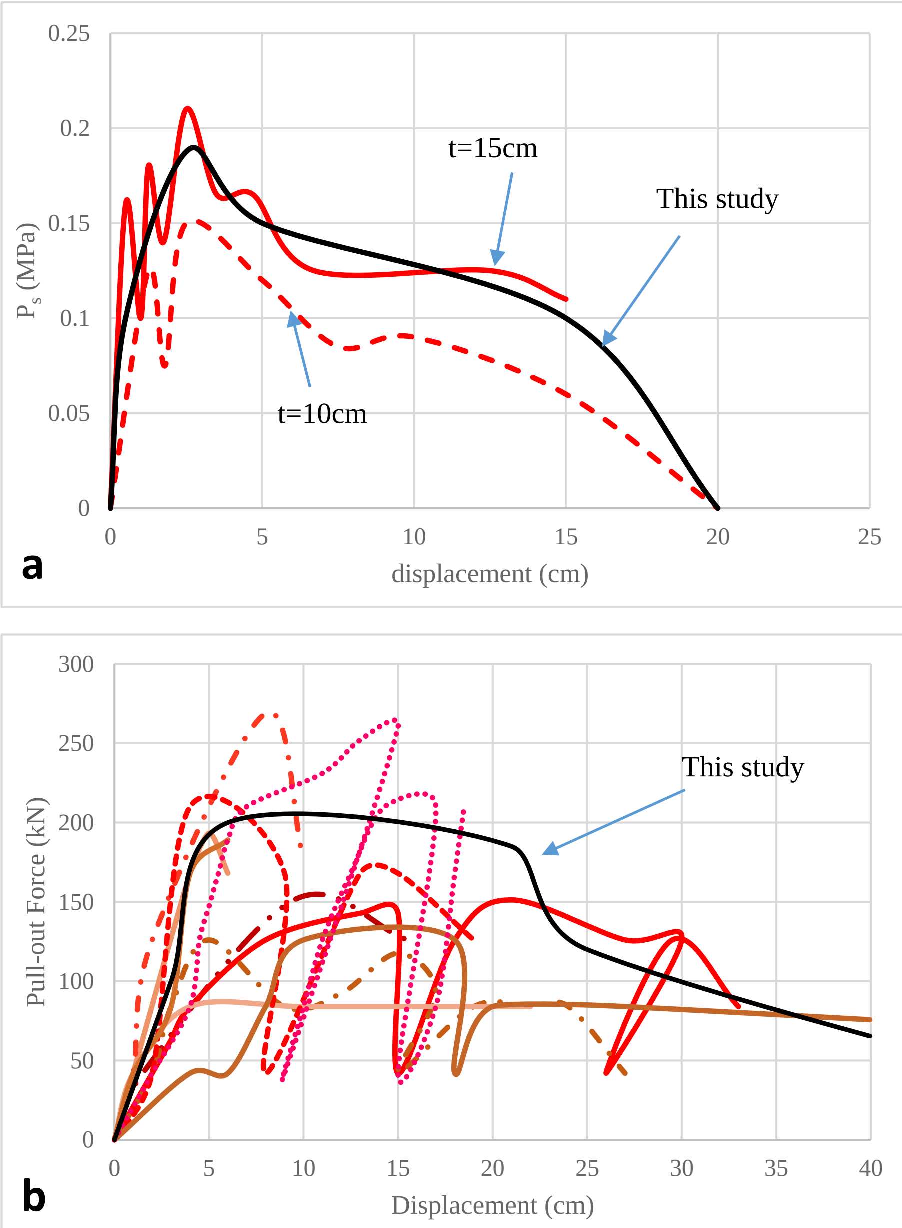

Fig. 10 Support pressure and displacement relationships for **a** shotcrete with wire mesh from Kirsten (1993), Stacey et al. (1995) and **b** cable bolt

a well-known EFNARC (1995) panel test, comes to mind. In fact, it is a simply supported point load test, it does not reflect the actual behaviour of a continuous liner (Bernard 1998) and it cannot be used for support design purposed directly. Large scale tests conducted on shotcrete and wire mesh are taken into consideration (Kirsten 1993; Stacey et al. 1995). These tests are statically indeterminate uniform loading tests unlike simply supported single point plate loading tests and they are capable of representing field behaviour. According to their results, the initial yield occurs within a few millimetres and at 2.5 cm displacement, the peak capacity is fully mobilised. Eventually, load-carrying capacity persists for more than 15 cm (Fig. 10a). Even though steel fibre-reinforced shotcrete is famous for its energy absorption capacity, the

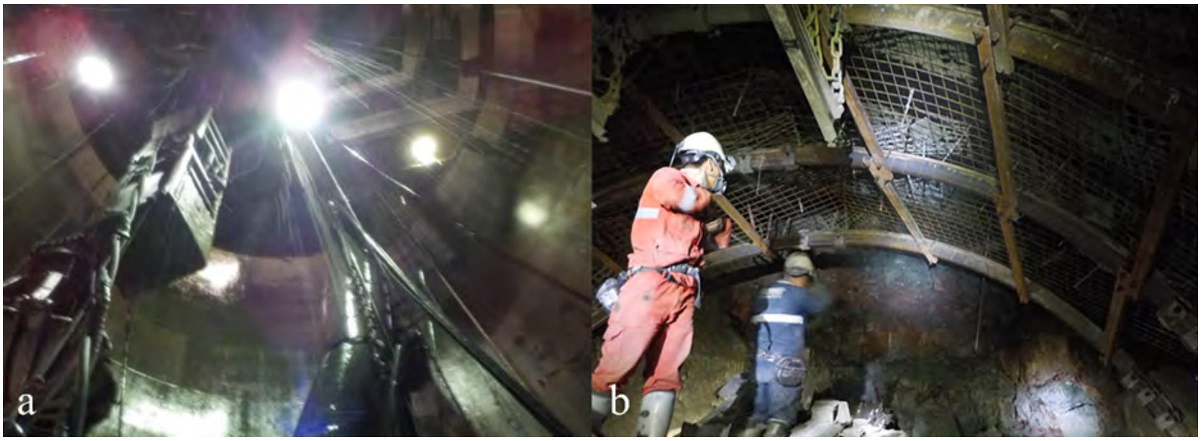

Fig. 11 A view inside the shaft (**a**), the decline heading (**b**), ground reaction and support response curves for thick reinforced concrete support (**c**), traditional roadway support (**d**), modified support system without a radial gap (**e**), proposed flexible support system with the radial gap (**f**)

residual capacity of the shotcrete with wire mesh is considerably high or even greater than the one with steel fibres having equal steel content (Carranza-Torres 2004).

Cable bolting is commonly called as rock reinforcement rather than rock support. The cable bolt used in the mine is a plain strand, resin grouted and has a minimum breaking capacity of 230kN. The bolts have a length of 6.3 m and minimum elongation at breakage is 21 cm. It is noticeable that the bolts are installed in weak rock units and their failure mechanism is majorly governed by the grout-rock interface and exceeding the breaking strength of the bolt is only a secondary concern. This may seem like a weakness, however, slippage of the rock bolt along the grout-rock interface enable energy dissipation to be developed. The pull-out test results of the bolts installed in the weak ground are presented in Fig. 6b. For some curves, unloading and loading cycles are visible due to zeroing of 15 cm stroke limit of the pull-out tester. In Fig. 10b, 10 cable bolt pull-out force vs. displacements are presented.

The abovementioned explanations were taken into account for the initial phase of the support system as well as for the support systems without invert. In the initial phase, the support ring is not closed and the support system had a shape similar to half-circle or horseshoe. In the initial phase, the support reaction differs from the analytical solution for circle-shaped support systems as explained above. However, during the second phase of the support system, invert construction is completed and a closed circle support system is ensured. In this phase, it was appropriate to consider the solution proposed by Carranza-Torres (2004). Similar to the closed support system in the roadway, a circular shaft concrete section was treated by the same method since it was a closed circle as it was installed once.

Conceptually diverse support systems were compared to each other by employing Ground Reaction Curves and Support Interaction Curves. A typical view of the shaft and decline heading is shown in Fig. 11.

The rigid support system consisting of 40 cm thick reinforced concrete with high early strength properties, stabilised the shaft opening having an inner diameter of 8 m. The rigid support system exhibited a stiff behaviour resulting in insignificant radial displacement and high-stress mobilisation, (Fig. 11c). The solution for support reaction is based on Carranza-Torres (2004).

Traditionally, 7 cm thick shotcrete and wire mesh were being applied together with cable bolting and steel arch. The response of the support system was insufficient as it can be inspected in Fig. 11d. The support reaction curves reveal that the support elements were in a yielded state.

Flexible support system consisting of 15 cm thick shotcrete and cable bolts allows a deformation around 20 cm. During this deformation, the deformation gap between bolted surface and steel arch converges. The application of the final layer of 15 cm thick shotcrete is delayed and the ground pressure acting on the

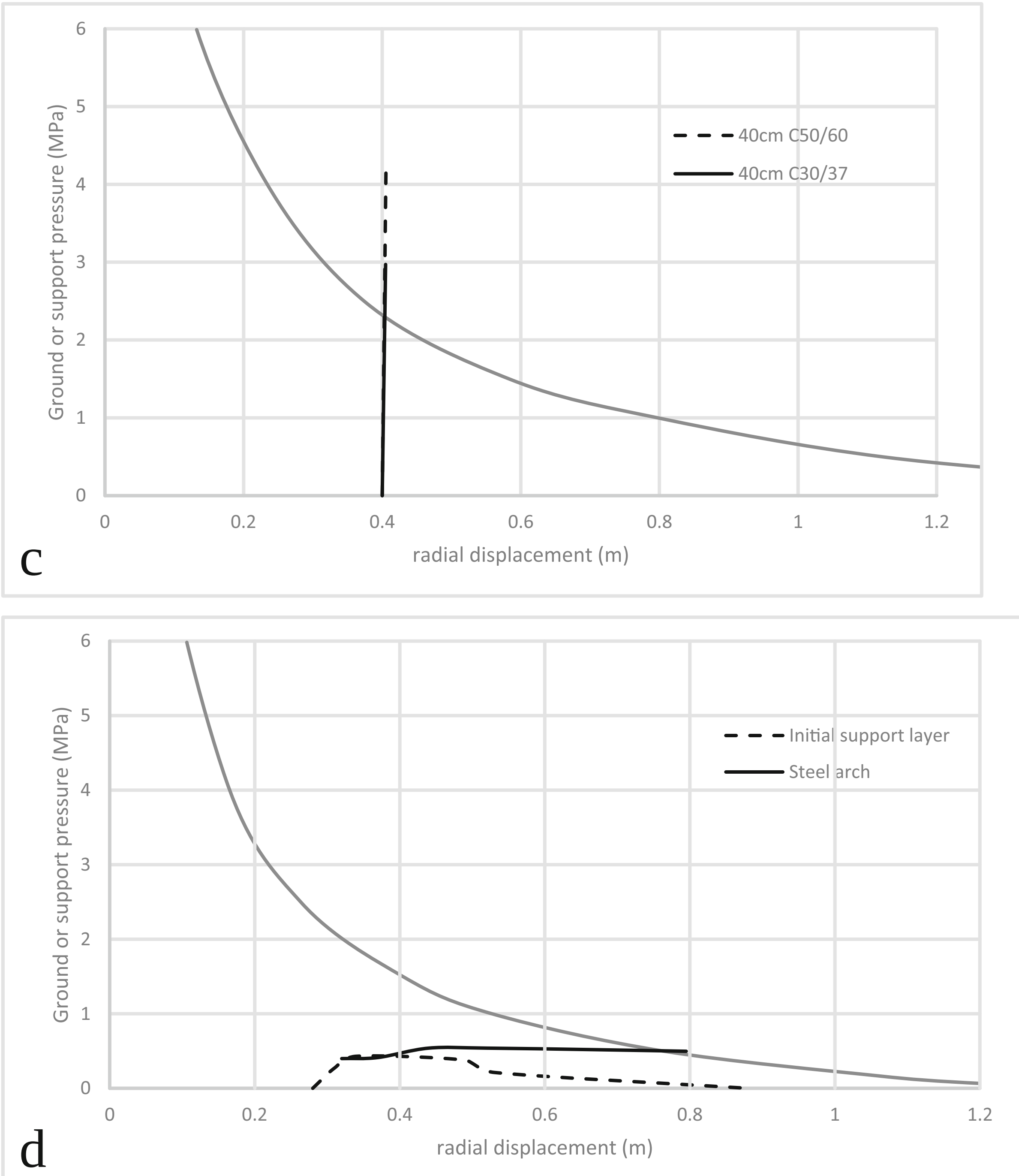

Fig. 11 continued

support is reduced by relaxation. Eventually, sufficient support pressure is established together with steel arches. However, the stabilisation is achieved after a radial displacement amount of 20 cm (Fig. 10f). The 20 cm value defines the deformation gap distance proposed in this study. When the radial gap is not included in the design, the overloading of the support system can be clearly presented in Fig. 11e.

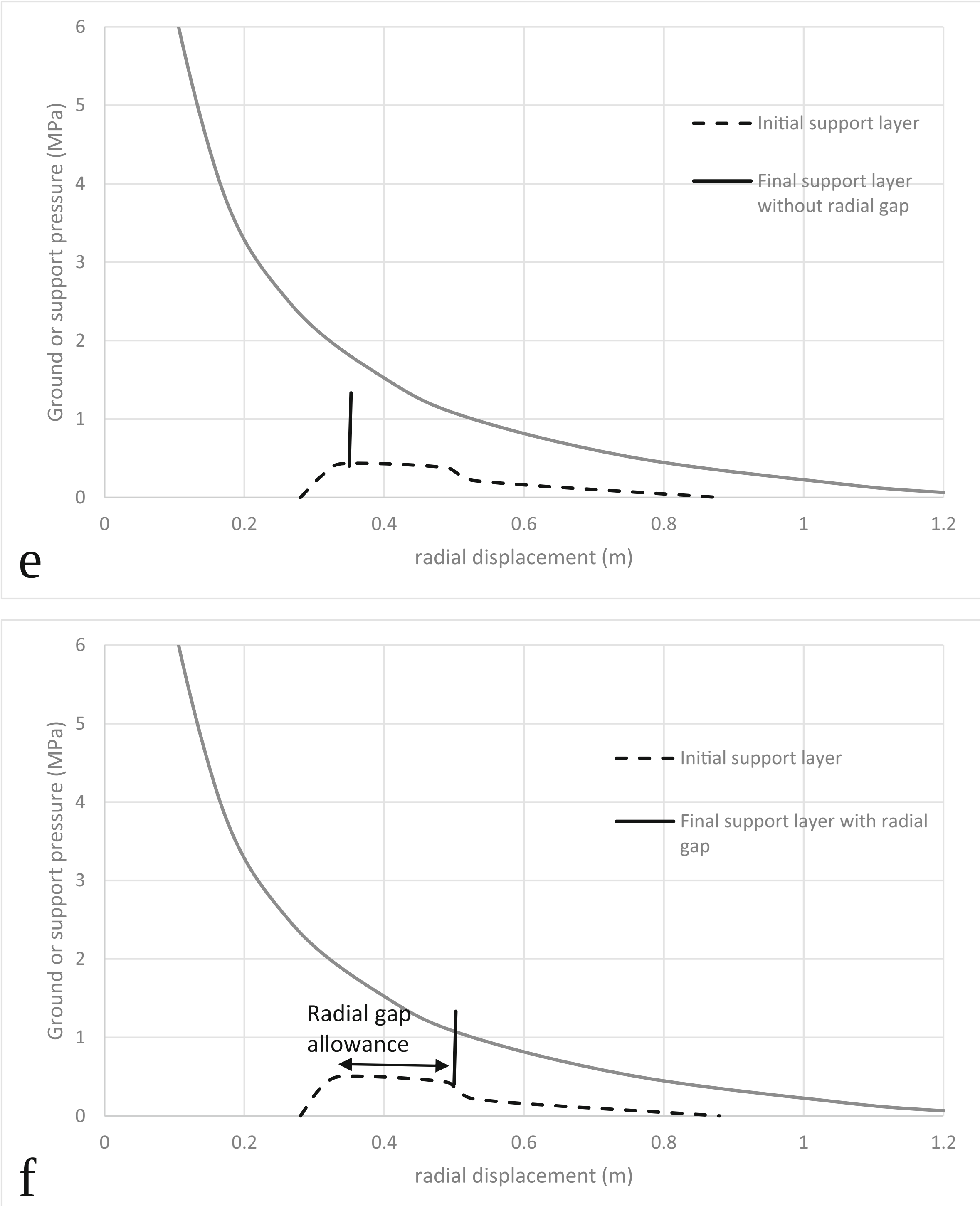

Fig. 11 continued

Support and ground reaction curves present balance which is satisfied by different support concepts. The heavy and rigid support concept has a support capacity of 3 MPa within a single day and above 4 MPa for 7 days. The reinforced concrete can sustain substantial support stressing and due to its stiff nature, a very insignificant convergence is allowed ($< 0.1\%$). The flexible and light support system for the decline with deformation gap has an initial support capacity of 0.544 MPa while the final shotcrete layer and steel arches satisfy a support pressure of 0.933 MPa. Although the initial system has a support capacity of 0.544 MPa, due to the insufficient capacity of shotcrete, the support capacity offered by the shotcrete is reduced and loads on the cable bolts are mobilised. Delayed installation of final shotcrete layer and delayed loading of the steel arch by the planned deformation gap, the opening can be stabilised at a mobilised support pressure around 1.2 MPa. Here, for the flexible support, delayed loading of the secondary elements plays an important role. If they were installed at the face, it is obvious that the support capacity would not be sufficient. However, as described in Sect. 4.2, some interval of the decline suffered excessive deformation since those chainages were lacking the final layer of shotcrete and closed support circle. Under these circumstances, provided support capacity falls down to a value smaller than 0.5 MPa. This low support pressure is beyond the deformation limits of the support and excessive deformation is allowed. This fact is also clearly visible in the ground-support reaction curves.

6 Conclusions

Squeezing problem encountered in a mine development was overcame by employing different support design procedures. The rigid support was constructed by a closed ring of 40 cm thick reinforced concrete having high early strength. The rigid support was able to resist the squeezing pressures without insignificant elastic deformation. This support constituted an example for conventional support.

The ground pressure can be considered as a function of underground opening deformation. Hence, radial displacement of the excavation boundary leads to a relaxation in the stressed rock mass which in turn result in a decrease in support load. In the flexible or yielding support systems, this concept is significantly beneficiated. In this research, a traditional support system had to be modified in order to prevent support from overstressing. A radial deformation gap was imposed on the support system which was consisting of commonly used support elements. Prediction of the deformation to be allowed is critical for a yielding support system as well as the system proposed in this research. The cross-sectional area is reduced during the deformation of the yielding support system hence, the deformation tolerance must be introduced to the excavation span in order to maintain the desired final cross-section. The deformation gap in the applied support system is capable of accommodating to a significant convergence (6–9%). When the ground reaction curves are taken into account, such high convergence magnitude is in the favour of rock pressure reduction. However, the deformation degrades the rock mass and in turn, can cause an increase in the plastic zone around the opening. During the yielding stage, the deformation should be allowed in a controlled manner thus avoiding degradation and loosening of the rock mass. Here, in this research, controlled deformation (yielding) is ensured by a thin shotcrete layer and cable bolts. Keeping the yielding pressure as high as possible is essential for such flexible-yielding and light support systems.

The study also reveals that the same ground conditions can be dealt with by different support systems with strongly diverse concepts. However, sometimes, the operational conditions may cause the effortful one to be used. It is noteworthy to tell that by using the conventional support elements, a very different solution can be proposed. Such solutions are important in mining since the modification of the support systems should be executed as fast as possible.

Acknowledgements The author thanks the management personnel of Polyak Eynez Energy Mining A.Ş. and Fina Energy for granting permission to use necessary data. The author presents his gratitudes to the engineering team of Polyak Eynez, for providing extensive data on the study area. The author exclusively thanks to Survey Engineer Mehmet Sarıtaş for his additional care of during data collection.

Compliance with ethical standards

Conflict of interest The authors declare that they have no conflict of interest.

References

Barla G (2001) Tunnelling under squeezing rock conditions. Eurosummer-school in tunnel mechanics, Innsbruck, pp 169–268

Barla G, Bonini M, Semeraro M (2011) Analysis of the behaviour of a yield-control support system in squeezing rock. Tunn Undergr Space Technol 26(1):146–154

Barton N, Lien R, Lunde J (1974) Engineering classification of rock masses for the design of tunnel support. Rock Mech 6(4):189–236

Bernard SE (1998) Flexural behaviour in square steel fibre reinforced concrete slabs. In: Proceedings of CONSEC'98 conference, Tromso, Norway

Bieniawski Z (1989) Engineering rock mass classifications. Wiley, New York

Brinkmann and Feist (1970) Soma dağlarının jeolojisi. Bull Miner Res Explor 74(74) (in Turkish)

Cantieni L, Anagnostou G (2009) The interaction between yielding supports and squeezing ground. Tunn Undergr Space Technol 24(3):309–322

Cao C, Shi C, Lei M, Yang W, Liu J (2018) Squeezing failure of tunnels: a case study. Tunn Undergr Space Technol 77:188–203

Carranza-Torres C (2004) Elasto-plastic solution of tunnel problems using the generalized form of the Hoek–Brown failure criterion. Int J Rock Mech Min Sci 41(SUPPL. 1):1–11

Cengiz O, Turanli L (2004) Comparative evaluation of steel mesh, steel fibre and high-performance polypropylene fibre reinforced shotcrete in panel test. Cem Concr Res 34(8):1357–1364

European Federation of Producers and Applications of Specialist Products for Structures (1996) European specification for sprayed concrete, EFNARC, Loughborough University, pp 8–10

Goel RK, Jethwa JL, Paithankar AG (1995) Indian experiences with Q and RMR systems. Tunn Undergr Space Technol 10(1):97–109

Guan K, Zhu W, Wei J, Liu X, Niu L, Wang X (2018) A finite strain numerical procedure for a circular tunnel in strain-softening rock mass with large deformation. Int J Rock Mech Min Sci 112:266–280

Hoek E (2001) Big tunnels in bad rock. J Geotech Geoenviron Eng 127(9):726–740

Hoek E (2007) Practical rock engineering—chapter 12: Tunnels in weak rock

Hoek E, Diederichs MS (2006) Empirical estimation of rock mass modulus. Int J Rock Mech Min Sci 43(2):203–215

Hoek E, Carranza-Torres C, Corkum B (2002) Hoek-Brown failure criterion-2002 edition. Proc NARMS-Tac 1(1):267–273

Høien AH, Nilsen B, Olsson R (2019) Main aspects of deformation and rock support in Norwegian road tunnels. Tunn Undergr Space Technol 86:262–278

Jimenez R, Recio D (2011) A linear classifier for probabilistic prediction of squeezing conditions in Himalayan tunnels. Eng Geol 121(3–4):101–109

Kahraman S, Aloglu AS, Aydin B, Saygin E (2019) The needle penetration index to estimate the performance of an axial type roadheader used in a coal mine. Geomech Geophys Geo-Energy Geo-Resour 5(1):37–45

Kirsten HAD (1993) Equivalence of mesh-and fibre-reinforced shotcrete at large deflections. Can Geotech J 30(3):418–440

Lowson AR, Bieniawski ZT (2013) Critical assessment of RMR based tunnel design practices: a practical engineer's approach. In: Proceedings of the SME, Rapid excavation and tunnelling conference, Washington, DC, USA, pp 23–26

Maden Tetkik Arama Genel Müdürlüğü (General Directorate of Mineral Research and Exploration), Earth Sciences Map Viewer and drawing tool. Website: https://yerbilimleri.mta.gov.tr/anasayfa.aspx Online acces: 12.05.2020

Majumder D, Viladkar MN, Singh M (2017) A multiple-graph technique for preliminary assessment of ground conditions for tunneling. Int J Rock Mech Min Sci 100:278–286

Mezger F, Ramoni M, Anagnostou G, Dimitrakopoulos A, Meystre N (2017) Evaluation of higher capacity segmental lining systems when tunnelling in squeezing rock. Tunn Undergr Space Technol 65:200–214

Mezger F, Ramoni M, Anagnostou G (2018) Options for deformable segmental lining systems for tunnelling in squeezing rock. Tunn Undergr Space Technol 76:64–75

Nebert K (1978) Lignite-bearing Soma Neogene area, western Turkey. Bull Direct Min Res Explor 90:20–70

Öge İF (2017) Prediction of cementitious grout take for a mine shaft permeation by adaptive neuro-fuzzy inference system and multiple regression. Eng Geol 228:238–248

Öge İF (2018) Prediction of top coal cavability character of a deep coal mine by empirical and numerical methods. J Min Sci 54(5):793–803

Öge İF, Yazar R, Yazar MA, Hür A, Tarhan Ş, Göle M (2019) The implementation of a multi-layer support system in an excessively deformed roadway. In: Proceedings of International Mining Congress and Exhibition of Turkey, 16–19 April 2019, Antalya/Turkey, pp 239–246

Perera MSA, Ranjith PG, Choi SK, Bouazza A, Kodikara J, Airey D (2011) A review of coal properties pertinent to carbon dioxide sequestration in coal seams: with special reference to Victorian brown coals. Environ Earth Sci 64(1):223–235

Rocscience Inc., Phase2 Software v.8.0, (2011).

Shen B (2014) Coal mine roadway stability in soft rock: a case study. Rock Mech Rock Eng 47(6):2225–2238

Stacey TR, OrtIepp WD, Kirsten HAD (1995) Energy-absorbing capacity of reinforced shotcrete, with reference to the containment of rockburst damage. J South Afr Inst Min Metall 95(3):137–140

Stille H, Palmström A (2008) Ground behaviour and rock mass composition in underground excavations. Tunn Undergr Space Technol 23(1):46–64

Tian H, Chen W, Yang D, Wu G, Tan X (2016) Numerical analysis on the interaction of shotcrete liner with rock for yielding supports. Tunn Undergr Space Technol 54:20–28

Ulusay R, Hudson JA (2007) The Blue Book-The complete ISRM suggested methods for rock characterization, testing and monitoring: 1974–2006. ISRM and Turkish National Group of ISRM, Ankara

Vishwakarma AK, Behera T, Rai R et al (2020) Impact assessment of coal mining induced subsidence on native soil of South Eastern Coal Fields: India. Geomech Geophys Geo-energ Geo-resour 6:31. https://doi.org/10.1007/s40948-020-00156-y

Vlachopoulos N, Diederichs MS (2009) Improved longitudinal displacement profiles for convergence confinement analysis of deep tunnels. Rock Mech Rock Eng 42(2):131–146

Wasantha PLP, Ranjith PG, Zhao J, Shao SS, Permata G (2015) Strain rate effect on the mechanical behaviour of sandstones with different grain sizes. Rock Mech Rock Eng 48(5):1883–1895

Zhang JZ, Zhou XP (2017) Time-dependent jamming mechanism for Single-Shield TBM tunneling in squeezing rock. Tunn Undergr Space Technol 69:209–222

Zhang H, Elsworth D, Wan Z (2018) Failure response of composite rock-coal samples. Geomech Geophys Geo-energ Geo-resour 4:175–192. https://doi.org/10.1007/s40948-018-0082-x